

Volume Relaxation Far from Equilibrium

GEORGE W. SCHERER*[†]

Research and Development Division, Corning Glass Works, Corning, New York 14831

Narayanaswamy's model of structural relaxation is applied to the data of Hara and Suetoshi on volume relaxation in plate glass. Both the Adam-Gibbs and Arrhenius equations are used to represent the relaxation time. Equally good fits are obtained with both equations, but only the Adam-Gibbs model gives physically meaningful fitting parameters. The exponent b describing the shape of the relaxation time spectrum decreases at small values of reduced time, as it does for stress relaxation. Discrepancies between calculated and measured densities at 350°C are not resolved by allowing for a nonlinear driving force or thermorheological complexity.

I. Introduction

FOLLOWING a change in temperature, the properties of a viscous liquid are observed to change with time long after the sample has reached thermal equilibrium. This process, called structural relaxation, reflects the time required for the structure to rearrange into its new equilibrium configuration. The kinetics of structural relaxation have been studied in all classes of glass-forming liquids (polymers, oxides, salts, simple molecules, and metallic alloys).^{1,2} In studies of optical, electrical, and thermal properties, the data have been successfully described using a model introduced by Narayanaswamy.³ There is assumed to be a distribution of relaxation times exhibiting thermorheological simplicity; i.e., the shape of the distribution is independent of temperature. Following Tool,⁴ each relaxation time, τ , is assumed to depend on both the temperature, T , and the fictive temperature, T_f . The form of that dependence has recently been discussed in detail.⁵

Most of the tests of Narayanaswamy's model have been conducted at modest departures from equilibrium. To test the range over which thermorheological simplicity (TRS) applies, and to establish the proper form for $\tau(T, T_f)$, it is necessary to study a wide range of T and T_f . Fortunately, some excellent data for volume relaxation in a soda-lime-silicate plate glass have been reported by Hara and Suetoshi.^{6,†} In this paper, their data are analyzed in terms of Narayanaswamy's model. The Adam-Gibbs equation is shown to represent $\tau(T, T_f)$ better than the Arrhenius equation, and some departure from TRS is indicated at very low temperatures.

The experiments performed by Hara and Suetoshi⁶ are described in Section II. The theory of structural relaxation and the fitting procedure are described in Section III, and the results are presented in Section IV. Discrepancies between theory and experiment are discussed in Section V, and the conclusions are summarized in Section VI.

II. Experiments by Hara and Suetoshi

The material studied by Hara and Suetoshi⁶ was a plate glass whose (analyzed) composition is given in Table I. Unfortunately, no data were reported on the thermal expansion coefficient of the glass, and only one viscosity datum was provided. Samples in the form of plates, with dimensions 10 by 10 by 2 mm, were treated

in an electric furnace controlled to within 1°C of the desired temperature. When samples were inserted, the furnace temperature would drop slightly, then overshoot by 3° to 4°C, and return to the soak temperature in ≈ 3 min. The density of the samples was measured using a gradient column containing a mixture of bromoform and pentachloroethane. The sample and a standard were placed in the column and the temperature was adjusted until each passed a fixed line on the column. Using the difference between the temperatures (measured to within 0.01°C) at which each passed the mark, together with the known thermal expansion coefficient of the liquid, the density of the sample was calculated to an accuracy of 1×10^{-4} g/cm³.

Samples were equilibrated for long periods of time at temperatures of 516°, 530°, and 542°C and then removed quickly from the furnace. Since the viscosity of this glass is 10^{12} Pa·s at 543°C, these samples could not have changed their structure significantly during cooling. Therefore, the fictive temperatures, T_f , of these samples must also be very near 516°, 530°, and 542°C, respectively. From the densities of these samples, the following relation between T_f and density at room temperature, ρ (g/cm³), is obtained:

$$T_f (\text{°C}) = 585 - 6643(\rho - 2.4900) \quad (1)$$

According to this equation, the uncertainty of $\pm 1 \times 10^{-4}$ g/cm³ in ρ corresponds to ± 0.66 °C in T_f . A group of samples (designated "quenched") was equilibrated at 565°C for 10 min and then cooled in air; the result was $\rho = 2.4938$ g/cm³, which means, according to Eq. (1), that $T_f = 559.8$ °C, so relatively little change in structure occurred during cooling. Another group of samples (designated "annealed") was annealed at 500°C for 20 h to obtain $\rho = 2.5021$ g/cm³ ($T_f = 504.6$ °C), while others were held for 60 h to obtain $\rho = 2.5027$ g/cm³ ($T_f = 500.6$ °C). The change in density with time was measured for both quenched and annealed glasses at 516°, 530°, and 542°C; the results are represented by the circles in Fig. 1. The error bars on the curves represent the uncertainty of $\pm 1 \times 10^{-4}$ g/cm³ in the density measurement.

A set of experiments was done with samples that had received three different quenching treatments. Those designated "sample I" were held at 700°C for 5 min and then dropped into molten sodium nitrate at 320°C; these had $\rho = 2.4865$ g/cm³, $T_f = 608.3$ °C. Others, designated "sample II," were held at 570°C for 10 min and then cooled in air, to obtain $\rho = 2.4933$ g/cm³, $T_f = 563.1$ °C. Finally, those designated "sample III" were held at 540°C for 3 h and then cooled in air, to obtain $\rho = 2.4968$ g/cm³, $T_f = 539.8$ °C. The change in density with time was measured for all of these glasses during annealing at 500°, 450°, and 350°C. The results are presented in Figs. 2 and 3 for samples I, II, and III, respectively.

Table I. Glass Composition*

Oxide	Amount (wt%)
SiO ₂	71.6
Al ₂ O ₃	1.6
CaO	7.9
MgO	3.8
Na ₂ O	13.7
K ₂ O	0.5
TiO ₂	0.3
Fe ₂ O ₃	0.1
SO ₃	0.3

*From Ref. 6.

Received August 13, 1985; approved December 10, 1985.

[†]Member, the American Ceramic Society.

[†]Present address: E. I. du Pont de Nemours and Co., Central Research and Development Department, Experimental Station, 356/384, Wilmington, DE 19898.

[‡]An English translation of this paper is available from the American Ceramic Society: Order ACSD-199 from Data Depository Service, the American Ceramic Society, 65 Ceramic Drive, Columbus, OH 43214.

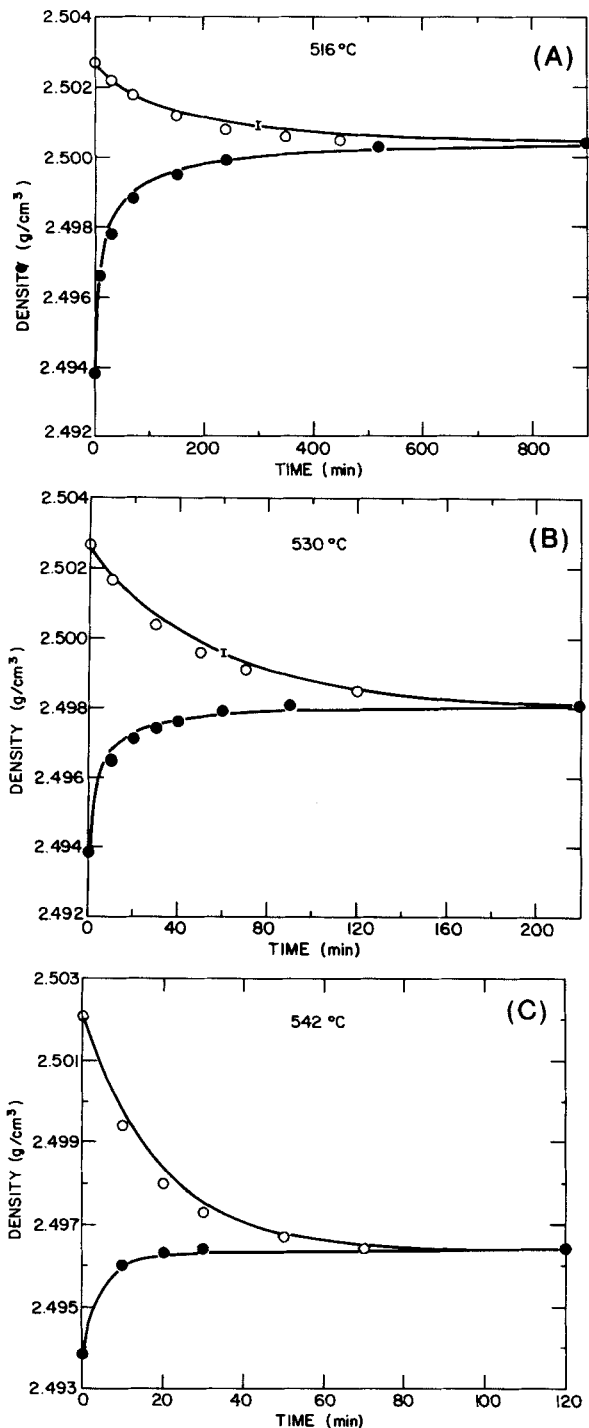


Fig. 1. Change in density with time at (A) 516°C, (B) 530°C, and (C) 542°C for (○) annealed and (●) quenched samples. Data from Ref. 6; solid lines from Eqs. (2), (3), and (11) with constants from fit to Adam-Gibbs model (Eq. (9)).

III. Theory

(1) Step Changes in Temperature

According to Narayanaswamy,³ if a glass is equilibrated at temperature T_1 and then suddenly exposed to temperature T_2 , ρ and T_f will change with time according to

$$\frac{\rho(t) - \rho_2}{\rho_1 - \rho_2} = \frac{T_f(t) - T_2}{T_1 - T_2} = M_v(\xi) \quad (2)$$

where ρ_1 and ρ_2 are the equilibrium densities corresponding to temperatures T_1 and T_2 , respectively, and $M_v(\xi)$ is the structural

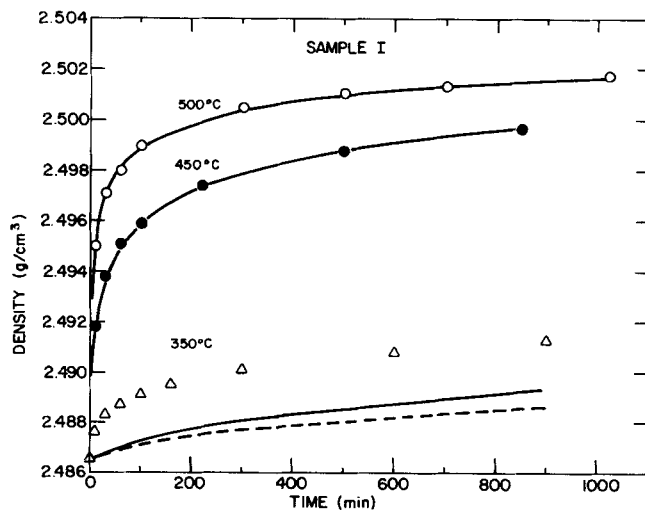


Fig. 2. Change of density with time for sample I at (○) 500°C, (●) 450°C, and (Δ) 350°C. Data from Ref. 6; calculations from Eqs. (11), (13), and (14) with constants from fit to (solid curves) Adam-Gibbs model (Eq. (9)) and (dashed curve) Arrhenius model (Eq. (4)).

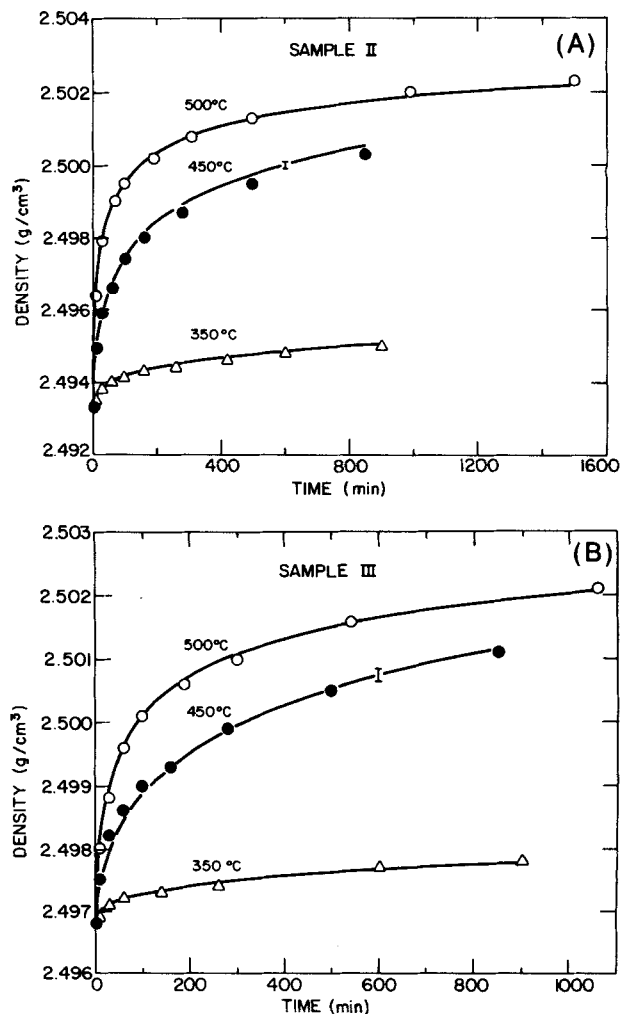


Fig. 3. Change of density with time for (A) sample II and (B) sample III at (○) 500°C, (●) 450°C, and (Δ) 350°C. Data from Ref. 6; solid lines from Eqs. (2), (3), and (11) with constants from fit to Adam-Gibbs model (Eq. (9)).

relaxation function for the volume. The reduced time, ξ , is defined by

$$\xi = \tau_{vr} \int_0^t \frac{dt'}{\tau_v} \quad (3)$$

where τ_v is the structural relaxation time for the volume (or density), τ_{vr} is the equilibrium value of τ_v at the arbitrary reference temperature T_r , and t is time. The relaxation time is related to temperature, T , and fictive temperature by

$$\tau_v = \tau_0 \exp \left[\frac{x\Delta H}{RT} + \frac{(1-x)\Delta H}{RT_f} \right] \quad (4)$$

where τ_0 is a constant, ΔH is the activation energy (generally found to be equal to that for viscous flow), R is the ideal gas constant, and x is a constant, $0 < x < 1$, that reflects the relative influence of temperature and structure (i.e., T_f) on the relaxation time. It has been argued² that a more appropriate expression for τ_v is the Adam-Gibbs equation:

$$\tau_v = \tau_0 \exp(A/TS_c) \quad (5)$$

The constant A is given by

$$A = \Delta\mu \ln W^* \quad (6)$$

where $\Delta\mu$ is the potential barrier hindering rearrangement and W^* is the number of configurations available to the smallest group of atoms that can undergo a cooperative rearrangement ($W^* \approx 2$). The configurational entropy, S_c , is given by

$$S_c(T_f) = \int_{T_2}^{T_f} (\Delta C_p/T) dT \quad (7)$$

where ΔC_p is the difference in heat capacity between the equilibrium liquid and the frozen glass. The upper limit of the integral is T_f rather than T , because the entropy depends on the actual structure of the glass, not its equilibrium structure. If ΔC_p is approximated by

$$\Delta C_p = B/T \quad (8)$$

where B is a constant, Eqs. (5) and (7) lead to

$$\tau_v = \tau_0 \exp \left[\frac{Q}{T(1 - T_2/T_f)} \right] \quad (9)$$

where $Q = AT_2/B$. At equilibrium, $T_f = T$ and Eq. (9) reduces to the Vogel-Fulcher-Tamman (VFT) equation

$$\tau_v = \tau_0 \exp[Q/(T - T_2)] \quad (10)$$

We will compare the performance of the Arrhenius model, Eq. (4), with that of the Adam-Gibbs (AG) model, Eq. (9). Hodge⁷ has made this comparison in a study of enthalpy relaxation in polymers and found that the AG model gave better fits to the data.

A commonly used form for the relaxation function is²

$$M_v(\xi) = \exp[-(\xi/\tau_{vr})^b] \quad (11)$$

where b is a constant. It should be noted that, for a given glass, each property may have a different relaxation time, τ_p , and relaxation function, M_p . However, for glasses similar to the one considered here, M_p and τ_p were found to be indistinguishable for volume and viscosity⁸ and for refractive index and enthalpy.⁹

The function in Eq. (11) is equivalent to a continuous distribution of relaxation times, but can be closely approximated by a set of discrete relaxation times, τ_i , as follows:¹⁰

$$M_v(\xi) = \sum_{i=1}^n w_i \exp(-\xi/\tau_{ir}) \quad (12)$$

The distributions corresponding to $b = 0.4$ and $b = 0.6$ are illustrated in Fig. 4. As b decreases, the distribution broadens so as to incorporate both faster and slower relaxation processes. It is generally difficult to measure the early portion of a relaxation curve ($M_v \geq 0.9$), so the fast relaxation processes are often not observed.

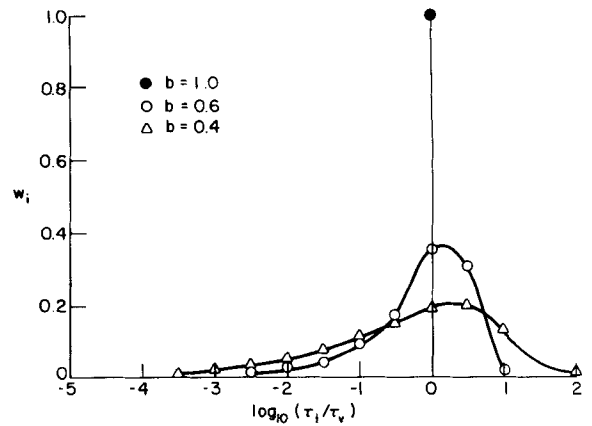


Fig. 4. Discrete spectrum of relaxation times (Eq. (12)) equivalent to continuous distribution (Eq. (11)) with (●) $b = 1.0$, (○) $b = 0.6$, and (△) $b = 0.4$.

In such cases, a distribution with a larger value of b , which neglects the processes with short relaxation times, will adequately represent the experimental data. However, when careful measurements are made, it is found¹¹⁻¹³ that the early portion of the relaxation curve, $M_v(\xi)$, requires a smaller value of b (≈ 0.3 to 0.4) than the later portion of the curve ($b \approx 0.5$ to 0.7). That is, a single value of b cannot describe the entire set of measurements, because the actual distribution of relaxation times characteristic of the glass is not the same as the distribution represented by Eq. (11). While this fact has been most convincingly demonstrated for stress relaxation,¹¹⁻¹³ similar behavior is probable for structural relaxation.

(2) Continuous Cooling

The second equality in Eq. (2) applies only for step changes in temperature that are so rapid that $T_f(0) = T_1$. All of the measurements by Hara and Suetoshi, except for the annealing of sample I, approximate that condition quite well. During the quenching of sample I, T_f decreases from $T_1 = 700^\circ\text{C}$ to $T_f = 608^\circ\text{C}$, and this thermal history must be taken into account. According to Narayanaswamy,³ we must write

$$T_f = T - \int_0^\xi M_v(\xi - \xi') \frac{dT}{d\xi'} d\xi' \quad (13)$$

to account for the change in T_f during cooling. Since ξ is a function of time, it continues to increase after the temperature stops changing, so $M_v \rightarrow 0$ and $T_f \rightarrow T$.

To apply Eq. (13) to the analysis of sample I, we must estimate the thermal history of the glass during quenching in the salt bath. If we assume that no large temperature gradient occurs in the thin (2 mm) glass plates, then the cooling rate of the sample after it is dropped into the salt bath at 320°C can be approximated by

$$dT/dt = -h[T(^\circ\text{C}) - 320] \quad (14)$$

where h is a heat-transfer coefficient. Given functions M_v and ξ , h is adjusted so that Eq. (13) gives $T_f = 608.3^\circ\text{C}$ when the sample has cooled to 320°C . The estimate of the cooling rate is complicated by the fact that the sample may have cooled well below 700°C before entering the salt bath. The most extreme assumption would be that the sample cooled in equilibrium to 608.3°C and then was instantly quenched by the bath. In that case, Eq. (2) would apply. The results of calculations based on these assumed thermal histories are compared in Section IV. The possible significance of tempering effects is discussed in Section V.

(3) Fitting Theory to Data

All of the measurements by Hara and Suetoshi, except for the annealing of sample I, should obey Eqs. (2) to (4) and (11). There

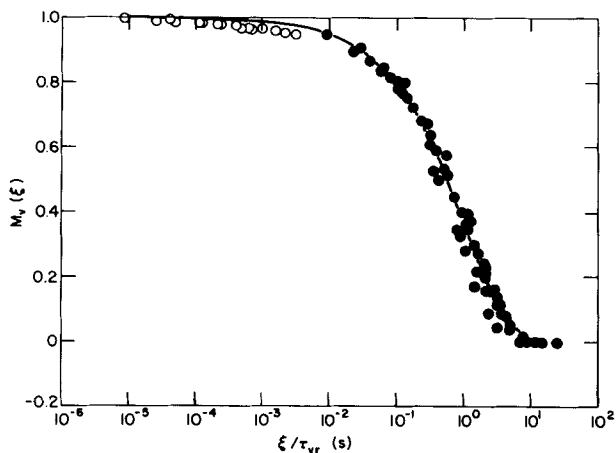


Fig. 5. Relaxation function M_v . Solid curve calculated using best-fit parameters for Adam-Gibbs model ($b = 0.64$); symbols represent all data (Ref. 6) except those for sample I; open circles represent samples II and III at 350°C.

are four fitting parameters at our disposal ($\tau_0, x, \Delta H, b$) which must be found by trial and error. A computer program was written to perform the indicated calculations, compare the results to the data, and adjust the parameters to improve the fit. The fitting was done using the Nelder-Mead¹⁴ algorithm. Equation (2) is non-linear, since $T_f(t)$ appears in ξ , so the solution must be obtained iteratively. For each time step, Δt , the change in reduced time, $\Delta \xi$, is estimated using the previous value of fictive temperature, T_f^- , and then a new value of fictive temperature, T_f^+ , is found from Eq. (2). Then a new estimate of $\Delta \xi$ is found using the average of T_f^- and T_f^+ , and another estimate of T_f^+ is obtained from Eq. (2). If Δt is small enough, no further iterations are required; for the present calculations, $\Delta t = 30$ s was found to be satisfactory.

A separate program was written to evaluate Eqs. (13) and (14) and was used as a subroutine in the Nelder-Mead program. For each set of parameters tested, the heat-transfer coefficient had to be chosen to give $T_f = 608.3^\circ\text{C}$ at the end of cooling. This was facilitated by the observation that

$$\frac{dT}{dt} \tau_v(608.3^\circ\text{C}) \approx \text{constant} \quad (15)$$

From Eq. (14), $dT/dt = -h(608.3 - 320)$, and the constant was found to be -130°C , so

$$h = 0.44/\tau_v(608.3^\circ\text{C}) \approx 0.4 \text{ to } 0.6 \text{ s}^{-1} \quad (16)$$

where τ_v is the equilibrium ($T_f = T$) relaxation time. The calculation simulated quenching to the hold temperature of 350°, 450°, or 500°C, followed by an isothermal hold. The time step for the calculation was chosen so that the change in T_f was no greater than 0.5°C in each step. The fitting program attempted to minimize the root-mean-square (rms) error in the calculated densities for all of the data simultaneously. Further mathematical details are provided in the appendices.

IV. Results

Initially, all of the data were fitted simultaneously, but it became evident that samples annealed at 350°C required a distinct set of fitting parameters. Therefore, the data for samples I, II, and III at 350°C were fitted separately; they are discussed in Section IV(2).

(1) Data at $T > 350^\circ\text{C}$

Equally good fits were obtained using the Arrhenius and AG forms for $\tau(T, T_f)$. The parameters for the fit using Eq. (4) were $\tau_0 = 3.9 \times 10^{-37}$ (s), $\Delta H/R = 73.0 \times 10^3$ (K), $x = 0.45$, and $b = 0.62$. The total rms error in the calculated densities was

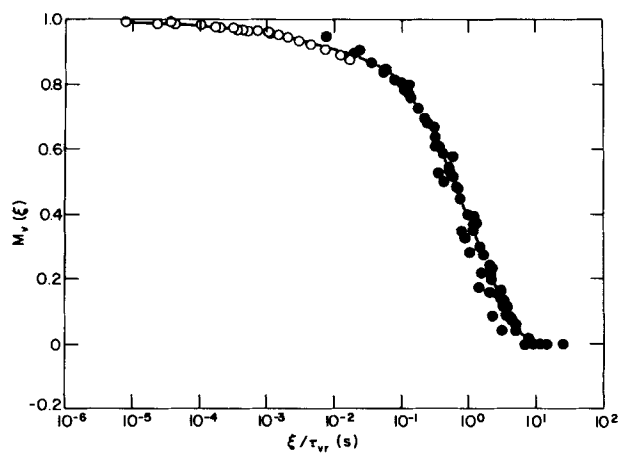


Fig. 6. Relaxation function M_v (curve fit through data (Ref. 6) in Fig. 5 and ξ values then recalculated); open circles represent samples I, II, and III at 350°C.

1.79×10^{-4} g/cm³; the experimental uncertainty was $\pm 1 \times 10^{-4}$ g/cm³. The parameters for the fit using Eq. (9) were $\tau_0 = 2.6 \times 10^{-15}$ (s), $Q = 1.49 \times 10^4$ (K), $T_2 = 436$ (K), and $b = 0.64$; the total rms error for the fit was 1.81×10^{-4} g/cm³.

The calculated relaxation function is shown in Fig. 5 along with all of the data except sample I. The curve is for the AG fit, but the curve for the Arrhenius fit is virtually identical. The solid curves in Figs. 1 to 3 were calculated using Eqs. (2), (3), and (11) with τ_v from the AG model, Eq. (9). Each plot includes an error bar corresponding to the reported experimental uncertainty in the density measurement. The calculated curves generally agree with the data within the experimental error.

(2) Measurements at 350°C

The open circles in Fig. 5 represent the data for samples II and III at 350°C, which were excluded from the fit. They clearly fall below the calculated curve. The error seems small, but the samples are so far from equilibrium that a small error in M_v causes a large error in ρ . The data in Fig. 5 can be fitted to a sum of exponential terms, as in Eq. (12), with the result shown in Fig. 6. The open circles now include the data for sample I at 350°C (treated as if the glass were initially equilibrated at 608.3°C and then annealed at 350°C). Now all of the data define a single curve. The portion corresponding to $\xi/\tau_vr < 10^{-2}$ can be fitted to Eq. (11) with $b \approx 0.4$, while the remainder requires $b \approx 0.63$. This increase in b with ξ is the same behavior observed for the stress relaxation function.¹¹⁻¹³

The solid curves for the 350°C data in Figs. 2 and 3 were calculated using M_v from Fig. 6 (based on 10 exponential terms) with τ_v from the AG model. The agreement is good for samples II and III, but seriously in error for sample I. The dashed curve in Fig. 2 is for the Arrhenius model, which gives even poorer agreement with sample I at 350°C (hereafter called I350).

The dashed curves in Fig. 7 were calculated from Eqs. (13) and (14) using the AG model and M_v from Fig. 6. Note that the fit to I450 is not as good as in Fig. 2 because of the use of the "corrected" relaxation function. The calculated relaxation is still much too slow. The assumed cooling rate could be at fault, so we need to consider what thermal history would give the most rapid relaxation for I350.

When the relaxation function is represented by Eq. (12), it is convenient to think of each exponential term as representing the relaxation of a particular "ordering parameter."¹⁵ The ordering parameter i is associated with a partial fictive temperature T_{fi} whose relaxation rate is controlled by relaxation time τ_i . The average fictive temperature is

$$T_f = \sum_{i=1}^n w_i T_{fi} \quad (17)$$

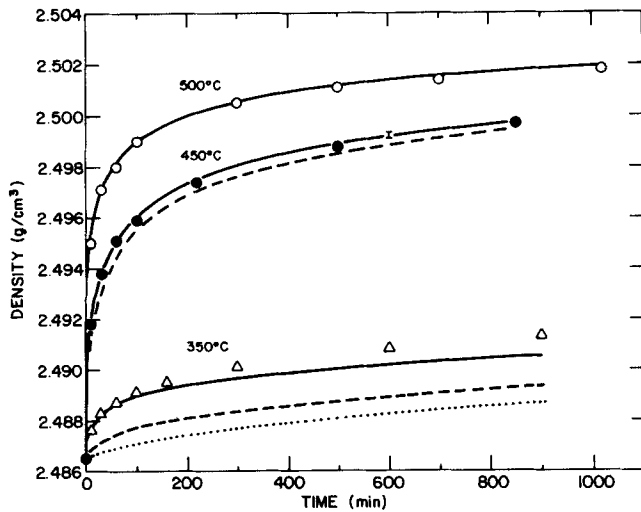


Fig. 7. Change of density with time for sample I. Data from Ref. 6; solid curves calculated using Adam-Gibbs model (Eq. (9)), with Eqs. (2), (3), and (12), assuming samples initially equilibrated at 608.3°C; calculations using Eqs. (12) to (14) shown by dashed curves (AG model) and dotted curve (Arrhenius model).

where the w_i are the same weighting factors that appear in Eq. (12). As a sample cools, the T_{fi} for the fast processes (or, rapidly relaxing order parameters) remain in equilibrium with T down to relatively low temperatures, while the T_{fi} for slow processes freeze at relatively high temperatures. Therefore, the T_{fi} for the fast processes are lower than the average T_f , and the T_{fi} for the slow processes are higher. The closer the "fast" T_{fi} are to T_f (they cannot be greater than T_f after cooling), the faster the sample can relax during a subsequent hold. Therefore, if we let all of the $T_{fi} = T_f = 608.3^\circ\text{C}$ for sample I, we get the most rapid relaxation possible for a quenched sample. That is how the solid curves in Fig. 7 were obtained, and the relaxation of 1350 is still underestimated. Thus, the most extreme assumption about the thermal history cannot eliminate the disagreement. Other explanations are considered in Section V.

(3) Examination of the Fitting Parameters

The temperature dependence of the relaxation time is illustrated in Fig. 8. The solid curves represent the AG model and the dashed curves the Arrhenius model. The equilibrium ($T_f = T$) and non-equilibrium ($T_f = \text{constant}$) curves for the two models are indistinguishable for $T_f \leq 550^\circ\text{C}$. At higher temperatures the AG model displays decreasing slope, so that the equilibrium value of τ_v is higher than for the Arrhenius model. However, the slope of the nonequilibrium curve also decreases, so upon extrapolation along $T_f = 608^\circ$ to 350°C , τ_v is lower than for the Arrhenius model. This is the effect that gives the slightly improved fit to sample I at 350°C .

The calculated densification kinetics and the shape of the τ_v curve are similar for the Arrhenius and AG models, but the constants in the equations for τ_v are quite different. The pre-exponential constant for the Arrhenius equation (3.9×10^{-37} s) is absurdly small compared to any physical vibration frequency. Such values are generally found, however, in the analysis of structural

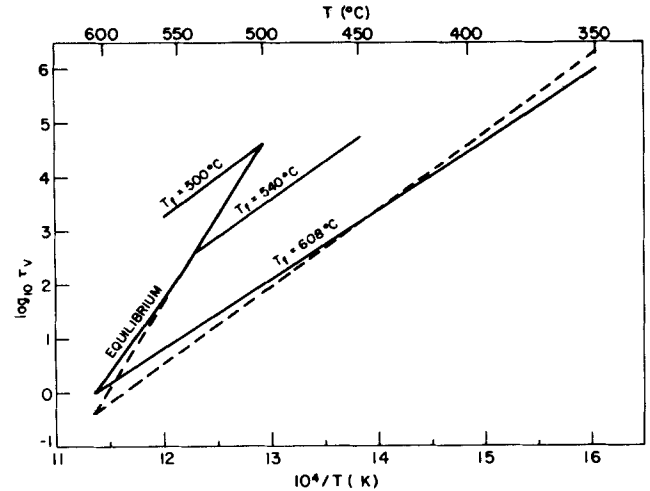


Fig. 8. Volume relaxation time vs. reciprocal temperature according to the AG model, Eq. (9) (solid curves), and Arrhenius model, Eq. (4) (dashed curves); the models are indistinguishable for $T_f \leq 550^\circ\text{C}$.

relaxation using this model. In contrast, the AG model gives $\tau_0 = 2.6 \times 10^{-15}$ s, which corresponds to an infrared vibration frequency.⁸ It is generally observed that the structural relaxation time has the same temperature dependence as the shear viscosity, η . Indeed, the activation energy (604 kJ/mol) for the Arrhenius model for τ_v is close to the value (≈ 630 kJ/mol) reported by Hara and Suetoshi⁶ for the viscosity of the glass near 540°C . The activation energy for the AG model is

$$\Delta H_{AG} \equiv R \frac{d \ln \tau_v}{d(1/T)} = \frac{RQ}{(1 - T_2/T)^2} \quad (18)$$

so it is temperature dependent, ranging from 783 kJ/mol at 450°C to 649 kJ/mol at 500°C to 558 kJ/mol at 550°C . It is clear from Fig. 8 that both models would agree well with the slope of the viscosity curve near 540°C . The viscosity of the glass is 10^{12} Pa·s at 543°C ,⁶ where τ_v is ≈ 280 s for either model. Therefore, the ratio is

$$\eta/\tau_v = 3.5 \times 10^9 \text{ Pa} \quad (19)$$

which is in the range typically observed.² Since τ_v and η have the same temperature dependence, Eq. (19) gives the ratio of the pre-exponential constants η_0 and τ_0 . Using τ_0 from the AG model one obtains the reasonable value $\eta_0 = 9 \times 10^{-6}$ Pa·s.

The constant Q in Eq. (9) is

$$Q = AT_2/B = (\Delta\mu)(\ln W^*)T_2/[T_g \Delta C_p(T_g)] \quad (20)$$

where the second equality follows from Eqs. (6) and (8). Using $T_g = 543^\circ\text{C} = 816$ K, $\Delta C_p(T_g) = 14.5$ J/mol (a typical value), $T_2 = 436$ K, and $Q = 1.49 \times 10^4$ K, Eq. (20) gives

$$\Delta\mu \ln W^* = 405 \text{ kJ/mol} \quad (21)$$

so if $W^* = 2$, then $\Delta\mu = 584$ kJ/mol (140 kcal/mol); if $\Delta\mu = 418$ kJ/mol (100 kcal/mol), then $W^* = 2.6$. These are physically reasonable values.

If the structure is frozen ($T_f = \text{constant}$), the activation energy for τ_v according to the Arrhenius model is $x\Delta H = 274$ kJ/mol (see Eq. (4)). For the AG model we find from Eq. (9) that

$$x_{AG} \Delta H_{AG} \equiv R \frac{d \ln \tau_v}{d(1/T)} \Big|_{T_f=\text{constant}} = \frac{RQ}{1 - T_2/T_f} \quad (22)$$

From Eqs. (18) and (22), the ratio of the nonequilibrium and equilibrium slopes at $T_f = T$ is

$$x_{AG} = 1 - T_2/T_f \quad (23)$$

⁸The concept of TRS requires that all of the τ_i in Eq. (12) have the same ΔH , so the distribution is achieved by adjusting the preexponential constant. Therefore, τ_{0i} for the shortest relaxation time is $\approx 10^9$ times smaller than τ_0 , which is not physically realistic. If all of the τ_i had the same τ_0 , the distribution could be produced by letting the activation energy vary. For $b \approx 0.6$, ΔH would only have to differ by ≈ 40 kJ/mol from the largest to the smallest τ_i (which differ by a factor of $\approx 10^3$). Such a small variation would preserve the appearance of TRS for all practical purposes, since a change in temperature of 150°C would increase the breadth of the distribution by a mere factor of 5.

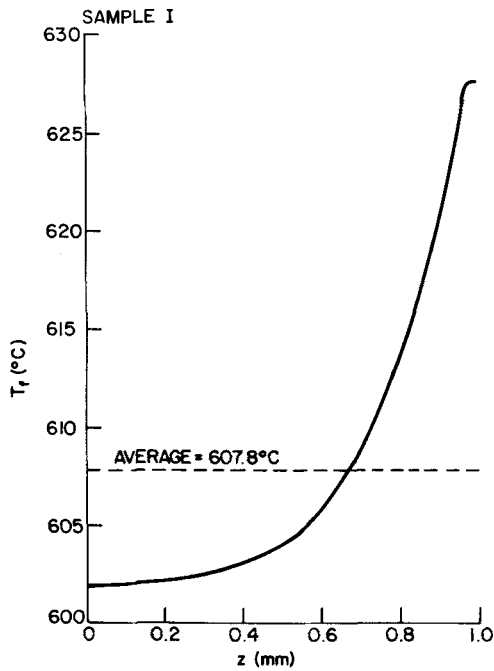


Fig. 9. Calculated variation of fictive temperature through thickness of plate in sample I after quenching; average density of entire sample corresponds to $T_f = 608^\circ\text{C}$.

which ranges from 0.506 when $T_f = 608^\circ\text{C}$ to 0.436 when $T_f = 500^\circ\text{C}$. This change in slope of the nonequilibrium curve is illustrated in Fig. 8.

V. Discussion

Narayanaswamy's model provides a good fit to the volume relaxation data of Hara and Suetoshi, except for the data at 350°C . In this section, we consider some possible reasons why the theory might fail for those samples.

(1) Shape of the Volume-Temperature Curve

Equation (1) implies that the thermal expansion coefficients of the liquid and glass (i.e., well above and well below T_g) are constant. In fact, a slight temperature dependence is expected.¹⁶ However, allowing for a reasonable temperature dependence forces a readjustment of all of the fitting parameters, and the fit to I350 is not improved.

(2) Tempering

Although the samples used by Hara and Suetoshi were only 2 mm thick, the surfaces of the plates would cool much faster than the interiors during quenching in the salt bath. Consequently, the surfaces would have lower densities¹⁷ (higher fictive temperatures) and would relax faster during annealing. To estimate the importance of this effect requires the use of a computer program to evaluate numerically the heat transfer from the sample and the simultaneous stress and structural relaxation. Using a program similar to that of Narayanaswamy and Gardon,¹⁸ which incorporates the structural relaxation model³ into the viscoelastic stress analysis developed by Lee, Rogers, and Woo,¹⁹ the quenching of sample I has been simulated.²⁰ As shown in Fig. 9, there is a substantial variation in T_f through the thickness of the plate. However, using the same program to simulate the annealing of sample I, we find that the average density of the sample changes at the rate predicted by Eq. (13) (solid lines in Fig. 2). The tempering has a surprisingly small influence on the relaxation of the average density, so it cannot account for the unexpectedly rapid relaxation of sample I.

(3) Nonlinear Behavior

Equation (13) is a generalization of Tool's⁴ equation

$$\frac{dT_f}{dt} = \frac{T - T_f}{\tau_v} \quad (24)$$

which means that the rate of structural relaxation is proportional to the departure from equilibrium, $T - T_f$. This linear proportionality may break down at large departures from equilibrium just as Hookean elasticity fails when a material is subjected to very large strains. For example, Ritland²¹ suggested a relation equivalent to

$$\frac{dT_f}{dt} = \frac{\pm(|T - T_f| + k|T - T_f|^N)}{\tau_v} \quad (25)$$

with $N = 2$; k is a constant. If k is small, the second term is significant only when $|T - T_f|$ is large. If we replace T_f with T_{fi} in Eq. (25) and fit it to the present data, the best fit is obtained with $k = 1 \times 10^{-13}$ and $N = 7$. Most of the data are adequately represented (for most, the additional term is negligible), but sample I at 350°C is underestimated by $\approx 6 \times 10^{-4} \text{ g/cm}^3$ at 10 to 60 min and overestimated by $\approx 5 \times 10^{-4}$ at 600 to 900 min. The short-time relaxation is governed by the fast processes for which $T_{fi} - T$ is relatively small (see Section IV(2)), and later relaxation is controlled by slower processes for which $T_{fi} - T$ is large. Therefore, the slower processes are disproportionately affected by Eq. (25). Thus, we have added two fitting parameters (k and N) without improving the fit significantly.

(4) Form of $\pi(T, T_f)$

Figure 9 shows that the slope of $\tau_v(T, T_f)$ given by the AG model allows for an improved fit to sample I at 350°C without degrading the fit for $T_f < 550^\circ\text{C}$. It may be that some other functional form would provide even greater curvature in τ_v between 550° and 608°C , so that $\tau_v(T_f = 608^\circ\text{C}, T = 350^\circ\text{C})$ would be small enough to account for the rapid relaxation observed experimentally. It has not been possible to obtain such behavior from the AG equation, even by allowing for an additional constant in Eq. (8).

Hara²² has suggested that the nonequilibrium portion of $\ln \tau_v$ is not linear in $1/T$, as it is for both models considered here, but is concave down. That would allow τ_v to be smaller at low temperatures and could account for the rapid relaxation at 350°C . It is not clear whether such temperature dependence could improve the fit to I350 without spoiling that for samples II and III at 350°C . At any rate, his theoretical justification is not persuasive. Direct measurements of the nonequilibrium viscosity by Mazurin *et al.*²³ showed no deviation from Arrhenian behavior; however, their data covered a smaller temperature range than that considered here.

(5) Thermorheological Complexity

Narayanaswamy's³ model is based on the assumption of thermorheological simplicity, which requires that the shape of the relaxation function be independent of temperature. This is a good approximation near T_g , but is not expected to be strictly true. For example, the relaxation time spectrum for B_2O_3 narrows dramatically at high temperatures.²⁴ This is to be expected when the various relaxation times have different activation energies. At low temperatures (not far from 350°C in some glasses), relaxation processes with small activation energies are observed, for example, in measurements of internal fraction.²⁵ Therefore, considering the wide range of T and T_f covered by Hara and Suetoshi,⁶ it is certainly plausible that there would be some variation in the distribution of relaxation times (i.e., in the shape of $M_v(\xi)$) with temperature.

Mazurin and Startsev²⁶ have suggested an extension of Narayanaswamy's³ model for cases when TRS is violated. They use Eq. (11), but let b be a linear function of T_f ; there is no theoretical basis for choosing the dependence of b on T and T_f . That model has not been tested against the present data.

It was noted earlier that the distribution of relaxation times can be produced by giving each τ_i the same (physically reasonable)

preexponential constant τ_0 , but varying the activation energy. Then the faster relaxation processes (smaller τ_i) have smaller ΔH_i . The result is that the distribution broadens as T decreases, because the large τ_i increase faster than the small τ_i . This is roughly equivalent to letting b decrease with T , except that it may not be possible to represent M_v by Eq. (11) at all temperatures. A model of this kind, discussed in Appendix C, was applied to the present data. No set of parameters was found that improved the fit to I350 without degrading the fit to the other data.

VI. Conclusions

Narayanaswamy's³ model has been shown to be very successful in describing the volume relaxation data of Hara and Suetoshi.⁶ For fictive temperatures between 608° and 500°C and annealing temperatures between 542° and 450°C, the data are fitted nearly within experimental error, with the relaxation function described by Eq. (11) with $b \approx 0.63$. The fits are equally good when the relaxation time is represented by the Arrhenius or Adam-Gibbs equations. The AG model is preferred in that it provides physically reasonable fitting parameters and gives a better description of the equilibrium temperature dependence of τ_v .

All of the data for $T \geq 450^\circ\text{C}$ correspond to $M_v \leq 0.9$, and all of the data for $T = 350^\circ\text{C}$ correspond to $M_v \geq 0.95$. The latter can be fitted only if that region of M_v is represented by a smaller value of b (≈ 0.4). Such variation of b with ξ is anticipated on the basis of studies of stress relaxation, but has not previously been demonstrated in structural relaxation. Even allowing for the change in b (by using a sum of exponential terms for M_v), the relaxation rate of the quenched sample (I350) is underestimated. Much, but not all, of the discrepancy can be eliminated by allowing for the uncertainty in the thermal history, as shown in Fig. 7.

In an effort to bring the calculations at 350°C into complete agreement with the data, we have considered the influence of tempering effects, nonlinear driving force for relaxation, and thermorheological complexity. None of those adjustments to the theory allowed all of the data to be fitted using a single set of parameters. Alternative forms for the temperature dependence of the relaxation time, such as that suggested by Hara,²² may be appropriate. However, there is presently no theoretical foundation for forms other than those used in this study.

In summary, the existing theory is quite good for describing relaxation kinetics within $\approx 100^\circ\text{C}$ of T_g in oxide glasses. However, the parameters determined in that temperature range may not be useful for predicting relaxation at very low temperatures. There is clearly a need for more data of this kind to ensure that the discrepancies noted here are the fault of the theory rather than erroneous measurements. Valuable experiments of this kind, involving low-temperature anneals and reheating, have been done by Hodge²⁷ and by Moyihan *et al.*²⁸ Finally, there is an obvious need for improved understanding of the physics underlying the relaxation process, perhaps along the lines of the model suggested by Brawer,²⁹ to justify or correct the current phenomenological model.

APPENDIX A

Calculation of T_f

The first step in the evaluation of Eq. (13) is to approximate Eq. (11) by Eq. (12); the procedure is described in Appendix B. Then T_f is given by Eq. (17), and each T_{fi} obeys Tool's equation

$$\frac{dT_{fi}}{d\xi} = \frac{T - T_{fi}}{\tau_{ir}} \quad (\text{A-1})$$

or, in integral form

$$T_{fi} = T - \int_0^{\xi/\tau_{vr}} \exp\{-\lambda_i[\xi(T) - \xi(T')]/\tau_{vr}\} dT' \\ \equiv T - I_i \quad (\text{A-2})$$

where $\lambda_i = \tau_{vr}/\tau_{ir}$. If the cooling rate is $q = dT/dt$, then fol-

lowing time step $\Delta t^{(n)} = \Delta T^{(n)}/q^{(n)}$, the integral can be approximated by

$$I_i^{(n)} = \sum_{j=1}^n [T^{(j)} - T^{(j-1)}] \exp\{-\lambda_i[\xi^{(n)} - \xi^{(j-1)}]/\tau_{vr}\} \quad (\text{A-3})$$

$$I_i^{(n)} = [T^{(n)} - T^{(n-1)}] \exp\{-\lambda_i[\xi^{(n)} - \xi^{(n-1)}]/\tau_{vr}\} \\ + \exp\{-\lambda_i[\xi^{(n)} - \xi^{(n-1)}]/\tau_{vr}\} I_i^{(n-1)} \quad (\text{A-4})$$

Given that

$$I_i^{(n-1)} = T^{(n-1)} - T_{fi}^{(n-1)} \quad (\text{A-5})$$

and

$$[\xi^{(n)} - \xi^{(n-1)}]/\tau_{vr} = \Delta t^{(n)}/\tau_v^{(n)} \quad (\text{A-6})$$

Eq. (A-4) may be written as

$$I_i^{(n)} = [T^{(n)} - T_{fi}^{(n-1)}] \exp[-\lambda_i \Delta t^{(n)}/\tau_v^{(n)}] \quad (\text{A-7})$$

and Eq. (A-2) as

$$T_{fi}^{(n)} = T^{(n)} - [T^{(n)} - T_{fi}^{(n-1)}] \exp[-\lambda_i \Delta t^{(n)}/\tau_v^{(n)}] \quad (\text{A-8})$$

Equation (A-8) permits calculation of $T_{fi}^{(n)}$ directly from $T_{fi}^{(n-1)}$. In contrast, if Eq. (11) is used, all previous values of T_f must be used, and the calculation requires 1 to 2 orders of magnitude more computer time. When $\Delta t^{(n)}$ is small enough so that the exponential function can be approximated by

$$\exp[-\lambda_i \Delta t^{(n)}/\tau_v^{(n)}] = 1 - \lambda_i \Delta t^{(n)}/\tau_v^{(n)} \quad (\text{A-9})$$

then Eq. (A-8) reduces to the equation suggested by Markovskiy and Soules.³⁰

APPENDIX B

Approximation to Eq. (11)

As explained in Appendix A, it is more efficient to use Eq. (12) than Eq. (11) in computation, so we seek the constants w_i and λ_i in the approximation

$$\sum_{i=1}^n w_i \exp(-t/\tau_i) \approx \exp[-(t/\tau_v)^b] \quad (\text{B-1})$$

For the present calculations n was equal to 20. The w_i are found by specifying n values of t . Let $t = \tau_i$; then

$$e^{-(\tau_i/\tau_v)^b} = \sum_{i=1}^n w_i e^{-\tau_i/\tau_i} \quad (\text{B-2})$$

By letting $t = \tau_2, \tau_3, \dots, \tau_n$, we form n linear equations that fix the w_i . The relaxation times must cover a broad range that varies with b . By trial and error¹ it was found that for $0.25 \leq b \leq 0.9$, the error in M_v is ≤ 0.003 when the relaxation times are spaced at equal logarithmic intervals

$$\ln \tau_i = \ln \tau_1 + \left(\frac{i-1}{19}\right) \ln(\tau_{20}/\tau_1) \quad (\text{B-3})$$

and the smallest and largest relaxation times are

$$\tau_1/\tau_v = [0.025 \exp(-8.047b)]^{1/b} \quad (\text{B-4})$$

and

$$\tau_{20}/\tau_v = (12.47 - 12.33b)^{1/b} \quad (\text{B-5})$$

¹After this work was done, these constants were optimized using the Nelder-Mead routine to give the best fit for $0.2 \leq b \leq 0.9$. The results, given below, should be used in place of Eqs. (B-4) and (B-5):

$$\tau_1/\tau_v = [0.0157 \exp(-7.93b)]^{1/b}$$

$$\tau_{20}/\tau_v = (10.34 - 10.14b)^{1/b}$$

Equation (B-2) was solved using subroutine LEQT2F from the IMSL Fortran library;³¹ the 40 constants were obtained in ≈ 0.3 s for a given value of b . Any $w_i < 10^{-4}$ (including negative values) were set equal to zero and the constants were renormalized to sum to unity.

APPENDIX C

Thermorheological Complexity

Narayanaswamy's³ assumption of thermorheological simplicity requires that all of the relaxation times have the same activation energy. Therefore, when we make the approximation in Eq. (B-1), if τ_i is given by Eq. (4), then

$$\tau_i = \tau_{0i} \exp \left[\frac{x\Delta H}{RT} + \frac{(1-x)\Delta H}{RT_f} \right] \quad (\text{C-1})$$

where τ_{0i} is a constant. Thus, the τ_i differ from one another (and from τ_v) only in the preexponential constant. When the distribution is broad, this requires some of the τ_{0i} to be too small to represent realistic vibrational frequencies. If we abandon TRS, we can let all of the τ_i have the same preexponential factor, τ_0 , and achieve the distribution by varying the activation energy. Since the Arrhenius equation requires a value of τ_0 that is physically meaningless, we will examine only the AG model, Eq. (9).

Let us assume that M_v is given correctly by Eq. (11) at temperature T^* . Then the method of Appendix B can be used to find the distribution of τ_i at T^* . The results are represented by the ratios

$$\lambda_i = \tau_v(T^*)/\tau_i(T^*) \quad (\text{C-2})$$

If the τ_i are given by

$$\tau_i = \tau_0 \exp \left[\frac{Q_i}{T(1 - T_2/T_f)} \right] \quad (\text{C-3})$$

then at equilibrium at T^* (i.e., $T = T_f = T^*$)

$$\tau_i(T^*) = \tau_0 \exp[Q_i/(T^* - T_2)] \quad (\text{C-4})$$

If we define

$$\tau_v(T^*) = \tau_0 \exp[Q/(T^* - T_2)] \quad (\text{C-5})$$

then

$$\tau_i(T^*) = \tau_v(T^*)/\lambda_i = \tau_0 \exp \left[\frac{Q}{T^* - T_2} - \ln \lambda_i \right] \quad (\text{C-6})$$

Comparing Eqs. (C-4) and (C-6) we find

$$Q_i = Q - (T^* - T_2) \ln \lambda_i \quad (\text{C-7})$$

The fitting routine was modified to seek the parameters τ_0 , Q , T^* , T_2 , and b . The calculation of $T_f(t)$ was performed as described in Appendix A, except that Eq. (A-8) was modified to

$$T_f^{(n)} = T^{(n)} - [T^{(n)} - T_f^{(n-1)}] \exp[-\Delta t^{(n)}/\tau_i^{(n)}] \quad (\text{C-8})$$

where

$$\tau_i^{(n)} = \tau_0 \exp \left[\frac{Q_i}{T^{(n)}(1 - T_2/T_f^{(n-1)})} \right] \quad (\text{C-9})$$

Thus, a different reduced time

$$\xi_i = \tau_{ir} \int_0^t \frac{dt}{\tau_i} \quad (\text{C-10})$$

applies for each ordering parameter. Excellent fits could be obtained for sample I alone or for the other data alone, but not for all together. Parameters that gave good fits for the step changes in temperature would underestimate the relaxation rate of I350. The following parameters gave reasonably good fits for the step-change data (rms error in ρ of 1.93×10^{-4} g/cm³), and very good fits

for sample I at 450° and 500°C, but underestimated I350 by $\approx 13 \times 10^{-4}$ g/cm³: $\tau_0 = 9.7 \times 10^{-16}$ s, $Q = 1.50 \times 10^4$ K, $T_2 = 440$ K, $b(T^*) = 0.80$, $T^* = 1124$ K. These parameters give $b \approx 0.6$ at 530°C and $b \approx 0.4$ at 350°C, but the shape of M_v is not well described by Eq. (11). The fit is about as good as that obtained from the standard model with M_v from Fig. 6, but τ_0 is rather small.

Acknowledgments: In the course of this work, I have had helpful and encouraging discussions with Dr. Simon Rekhson of General Electric Co., Prof. C. T. Moynihan of RPI, Prof. C. A. Angell of Purdue, and Dr. M. Hara of Asahi Glass Co. Their interest and advice are greatly appreciated. I am indebted to Dr. Ian Hodge (Eastman Kodak) for recommending the form of the AG model (Eq. (9)) used here, and for showing me his results with that model before publication. I thank David Smith (Corning Glass) for his help in writing the fitting routines, and Dr. Walter Buehl for his calculation of the tempering effect.

References

- C. T. Moynihan, P. B. Macedo, C. J. Montrose, P. K. Gupta, M. A. DeBolt, J. F. Dill, B. E. Dom, P. W. Drake, A. J. Easteal, P. B. Elterman, R. P. Moeller, H. Sasabe, and J. A. Wilder, "Structural Relaxation in Vitreous Materials," *Ann. N.Y. Acad. Sci.*, **279**, 15-35 (1976).
- O. V. Mazurin, "Relaxation Phenomena in Glass," *J. Non-Cryst. Solids*, **25**, 130-69 (1977).
- O. S. Narayanaswamy, "A Model of Structural Relaxation in Glass," *J. Am. Ceram. Soc.*, **54** [10] 491-98 (1971).
- A. Q. Tool, "Relations between Inelastic Deformability and Thermal Expansion of Glass in Its Annealing Range," *J. Am. Ceram. Soc.*, **29** [9] 240-53 (1946).
- G. W. Scherer, "Use of the Adam-Gibbs Equation in the Analysis of Structural Relaxation," *J. Am. Ceram. Soc.*, **67** [7] 504-11 (1984).
- M. Hara and S. Suetoshi, "Density Change of Glass in Transformation Range," *Rep. Res. Lab., Asahi Glass Co., Ltd.*, **5** [2] 126-35 (1955).
- I. M. Hodge, "Nonlinearity in Amorphous State Relaxations," Paper 96; presented at the Symposium on Relaxation Processes in Liquids and Glasses, American Chemical Society National Meeting, Miami, April 1985.
- S. M. Rekhson, A. V. Bulavaeva, and O. V. Mazurin, "Changes in the Linear Dimensions and Viscosity of Window Glass During Stabilization," *Inorg. Mater. (Engl. Transl.)*, **7** [4] 622-23 (1971).
- H. Sasabe, M. A. DeBolt, P. B. Macedo, and C. T. Moynihan, "Structural Relaxation in an Alkali-Lime-Silicate Glass"; pp. 339-48 in Proceedings of the 11th International Congress on Glass, Prague, 1977, Vol. I.
- C. T. Moynihan, L. P. Boesch, and N. L. Laberge, "Decay Function for the Electric Field Relaxation in Vitreous Ionic Conductors," *Phys. Chem. Glasses*, **14** [6] 122-25 (1973).
- R. W. Douglas, P. J. Duke, and O. V. Mazurin, "On the Network Contribution to the Anelasticity of Glasses," *Phys. Chem. Glasses*, **9** [6] 169-78 (1968).
- S. M. Rekhson, N. O. Gonchukova, and M. A. Chernousov, "Creep and Stress Relaxation in Glass in and below Transition Region"; pp. 329-38 in Proceedings of the 11th International Congress on Glass, Prague, 1977, Vol. I.
- J. Perez, B. Duperray, and D. Lefevre, "Viscoelastic Behavior of an Oxide Glass Near the Glass Transition Temperature," *J. Non-Cryst. Solids*, **44**, 113-36 (1981).
- D. M. Olsson, "A Sequential Simplex Program for Solving Minimization Problems," *J. Qual. Technol.*, **6** [1] 53-57 (1974).
- C. T. Moynihan, A. J. Easteal, M. A. DeBolt, and J. Tucker, "Dependence of the Fictive Temperature of Glass on Cooling Rate," *J. Am. Ceram. Soc.*, **59** [1-2] 12-16 (1976).
- G. W. Scherer and S. M. Rekhson, "Model of Structural Relaxation in Glass with Variable Coefficients," *J. Am. Ceram. Soc.*, **65** [6] C-94-C-96 (1982).
- R. Gardon, "Thermal Tempering of Glass"; in *Glass Science and Technology*, Vol. 5, Edited by D. R. Uhlmann and N. J. Kreidl, Academic Press, New York, 1980.
- O. S. Narayanaswamy and R. Gardon, "Calculation of Residual Stresses in Glass," *J. Am. Ceram. Soc.*, **52** [10] 554-58 (1969).
- E. H. Lee, T. G. Rogers, and T. C. Woo, "Residual Stresses in a Glass Plate Cooled Symmetrically from Both Surfaces," *J. Am. Ceram. Soc.*, **48** [9] 480-87 (1965).
- W. M. Buehl, Corning Glass Works; private communication.
- H. N. Ritland, "Density Phenomena in the Transformation Range of a Borosilicate Crown Glass," *J. Am. Ceram. Soc.*, **37** [8] 370-78 (1954).
- M. Hara, "Viscous Flow and Relaxation Phenomena in Inorganic Glass," *J. Phys. (Orsay, Fr.)*, **12** [43] C9-431-C9-434 (1982).
- O. V. Mazurin, Yu. K. Startsev, and L. N. Potselueva, "Temperature Dependences of the Viscosity of Some Glasses at Constant Structural Temperature," *Sov. J. Glass Phys. Chem. (Engl. Transl.)*, **5** [1] 68-79 (1979).
- J. Tauke, T. A. Litovitz, and P. B. Macedo, "Viscous Relaxation and Non-Arrhenius Behavior in B₂O₃," *J. Am. Ceram. Soc.*, **51** [3] 158-63 (1968).
- W. A. Zdaniewski, G. E. Rindone, and D. E. Day, "The Internal Friction of Glasses," *J. Mater. Sci.*, **14**, 763-75 (1979).
- O. V. Mazurin and Yu. K. Startsev, "Calculation of the Structural Relaxation of Properties of Glassy Materials Where the Principle of Thermorheological Simplicity Is Not Observed," *Sov. J. Glass Phys. Chem. (Engl. Transl.)*, **7** [4] 274-79 (1981).
- I. M. Hodge, "Effects of Annealing and Prior History on Enthalpy Relaxation in Glassy Polymers, 4, Comparison of Five Polymers," *Macromolecules*, **16**, 898-902 (1983).
- C. T. Moynihan, A. J. Bruce, D. L. Gavin, S. R. Loehr, and S. M. Opalka, "Physical Aging of Heavy Metal Fluoride Glasses—Sub-T_g Enthalpy Relaxation in a ZrF₄-BaF₂-LaF₃-AlF₃ Glass," *Polym. Eng. Sci.*, **24** [14] 1117-22 (1984).
- S. A. Brawer, "Theory of Relaxation in Viscous Liquids and Glasses," *J. Chem. Phys.*, **81** [2] 954-75 (1984).
- A. Markovsky and T. Soules, "An Efficient and Stable Algorithm for Calculating Fictive Temperatures," *J. Am. Ceram. Soc.*, **67** [4] C-56-C-57 (1984).
- IMSL Library (1982), IMSL, Inc., NBC Building, 7500 Bellaire Blvd., Houston, TX 77036. □